Article

Doping of Polyaniline by Acid–Base Chemistry: Density Functional Calculations with Periodic Boundary Conditions

Adrin Varela-Ivarez, Jos A. Sordo, and Gustavo E. Scuseria

J. Am. Chem. Soc., **2005**, 127 (32), 11318-11327• DOI: 10.1021/ja051012t • Publication Date (Web): 23 July 2005

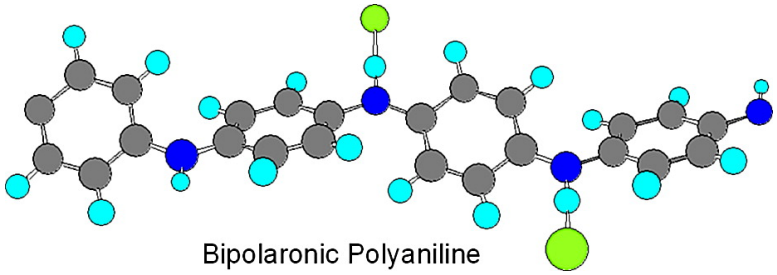

More About This Article

Additional resources and features associated with this article are available within the HTML version:

- Supporting Information
- Links to the 8 articles that cite this article, as of the time of this article download
- Access to high resolution figures
- Links to articles and content related to this article
- Copyright permission to reproduce figures and/or text from this article

View the Full Text HTML

J|A|C|S
ARTICLES
Published on Web 07/23/2005

Doping of Polyaniline by Acid−Base Chemistry: Density Functional Calculations with Periodic Boundary Conditions

Adrián Varela-Álvarez,[†] José A. Sordo,*[,†] and Gustavo E. Scuseria*[,‡]

Contribution from the Laboratorio de Química Computacional, Departamento de Química Física y Analítica, Facultad de Química, Universidad de Oviedo, 33006, Oviedo, Spain, and Department of Chemistry, Rice University, Houston, Texas 77005-1892

Received February 17, 2005; E-mail: jasg@uniovi.es

Abstract: Calculations with Gaussian orbitals and periodic boundary conditions using several density functionals are carried out to study the proton-doping of polyaniline. We explore previously proposed mechanisms to explain the spectacular increase of the electrical conductivity of polyaniline upon protonation. The structural and spectroscopic theoretical predictions for both polaron and bipolaron lattices agree quite well with the experimental data, and we find that the bipolaron structure is lower in energy.

1. Introduction

The discovery of conducting polymers and their doping over the full range from insulator to metal by Heeger, MacDiarmid, Shirakawa and co-workers[1,2] has been landmark research leading to what has been designated as the "fourth generation of polymer materials".[3,4] Polyaniline (PANI) is a family of polymers that represents the oldest electroactive synthetic material.[5,6] Its potential applications in organic lightweight batteries, microelectronics, and optical displays, among others,[7] as well as its significantly different properties than those of earlier studied materials such as polyacetylene,[8] are behind the great deal of attention received by this material in the recent literature.[7]

In the mid-1980s MacDiarmid and co-workers[9] showed that PANI can render conduction by protonation of the emeraldine base (**EB**) leading to emeraldine salt (**ES**) through acid−base chemistry. Heeger and co-workers proposed the use of functionalized protonic acids with the goal of making PANI processable in the conducting form.[10]

A number of theoretical studies have been devoted to study the electronic structure of PANI, including extended Hückel theory (EHT),[11] the Su−Shrieffer−Heeger model (SSH),[12] the valence effective Hamiltonian (VEH),[13] as well as molecular mechanics (MM), AM1, ZINDO, HF, DFT,[14] and MP2[15] calculations. All these studies focused on different oligomer structures of PANI. As a general conclusion, most of the methods are able to predict band gap structures that, once extrapolated to the infinite chain, are in reasonable agreement with the corresponding experimental values.

In a recent feature article,[4] Heeger has analyzed the doping mechanism of PANI by protonation according to the process presented in Scheme 1 in which, upon protonation, the semiconducting emeraldine base **EB** leads to the emeraldine salt **ESII** through a mechanism, originally proposed by MacDiarmid and co-workers,[16] involving a structural change with one unpaired spin per repeat unit but with no change in the number of electrons. **ESII** represents a potentially metallic material with a half-filled band. In terms of self-localized nonlinear excitations,[16−18] it is said that the protonation of **EB** leads to a spinless charged structure **ESI** (bipolaron), which rearranges to a charged radical open-shell structure **ESI′** (polarons) and finally splits into two **ESII** units (polaron). Heeger has concluded that: "*This remarkable conversion from semiconductor to metal has been well-described, but it is not well understood from the view of basic theory. There are no calculations showing that the metallic (emeraldine salt) final state is lower in energy than the semiconductor and there is no detailed understanding of the rearrangement reactions showed in Scheme 1*". This statement has prompted us to undertake a computational analysis on the different structures involved in MacDiarmid and co-workers' mechanism.

In this paper, we employ recently developed methodology,[19−23] especially suited for dealing with periodic systems such as the

[†] Universidad de Oviedo.
[‡] Rice University.

(1) Shirakawa, H.; Louis, E. J.; MacDiarmid, A. G.; Chiang, C. K.; Heeger, A. J. J. *Chem. Commun.* **1977**, 578.
(2) Chiang, C. K.; Fincher, C. R., Jr.; Park, Y. W.; Heeger, A. J.: Shirakawa, H.; Louis, E. J. *Phys. Rev. Lett.* **1977**, *39*, 1098.
(3) Ranby, B. In *Conjugated Polymers and Related Materials: The Interconnection of Chemical and Electronic Structures*; Salaneck, W. R., Lundström, I., Ranby, B., Eds.; Oxford University Press: Oxford, 1993; Chapter 3.
(4) Heeger, A. J. J. *Phys. Chem. B* **2001**, *105*, 8475.
(5) Fritzsche, J. *J. Prakt. Chem. (Leipzig)* **1840**, *20*, 454.
(6) Wudl, F.; Angus, R. O., Jr.; Lu, F. L.; Allemand, P. M.; Vachon, D. J.; Nowak, M.; Liu, Z. X.; Heeger, A. J. *J. Am. Chem. Soc.* **1987**, *109*, 3677.
(7) Liu, W.; Kuwer, J.; Tripathy, S.; Senecal, K. J.; Samuelson, L. *J. Am. Chem. Soc.* **1999**, *121*, 71 and references therein.
(8) McCall, R. P.; Ginder, J. M.; Leng, J. M.; Ye, H. J.; Manohar, S. K.; Masters, J. G.; Asturias, G. E.; MacDiarmid, A. G.; Epstein, A. J. *Phys. Rev. B* **1990**, *41*, 5202 and references therein.
(9) Salaneck, W. R.; Lunström, I.; Haung, W. S.; MacDiarmid, A. G. *Synth. Met.* **1986**, *13*, 291.
(10) Cao, Y.; Smith, P.; Heeger, A. J. *Synth. Met.* **1992**, *53*, 293.
(11) Euler, W. B. *Solid State Commun.* **1986**, *57*, 857.
(12) Ginder, J. M.; Epstein, A. J. *Phys. Rev. B* **1990**, *41*, 10674.
(13) Libert, J.; Cornil, J.; dos Santos, D. A.; Brédas, J. L. *Phys. Rev. B* **1997**, *56*, 8638.
(14) Kwon, O.; McKee, M. L. *J. Phys. Chem. B* **2000**, *104*, 1686.
(15) Lim, S. L.; Tan, K. L.; Kang, E. T.; Chin, W. S. *J. Chem. Phys.* **2000**, *112*, 10648.
(16) Stafström, S.; Brédas, J. L.; Epstein, A. J.; Woo, H. S.; Tanner, D. B.; Huang, W. S.; MacDiarmid, A. G. *Phys. Rev. Lett.* **1987**, *59*, 1464.
(17) Brédas, J. L.; Street, G. B. *Acc. Chem. Res.* **1985**, *18*, 309.
(18) Heeger, A. J.; Kivelson, S.; Schrieffer, J. R.; Su, W.-P. *Rev. Mod. Phys.* **1988**, *60*, 781.

10.1021/ja051012t CCC: $30.25

Scheme 1. McDiarmid and Co-Workers Proposed Mechanism (see Ref 16)[a]

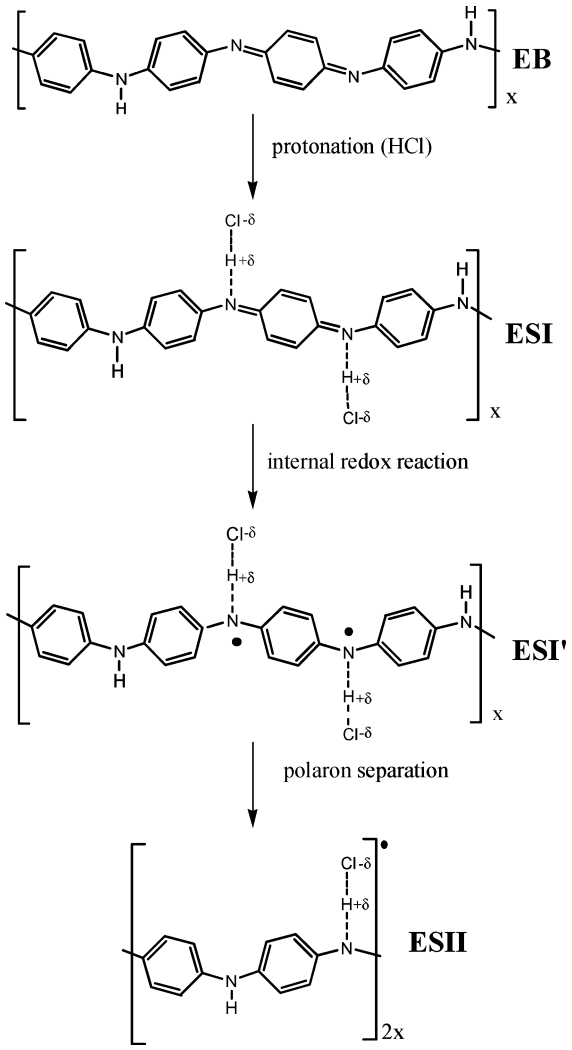

[a] $-\delta$ Represents a Negative Charge on the Counterion ($Cl^{-\delta}$) and $+\delta$ Represents the Counterbalancing Positive Charge Delocalized over the Chain.

ones in Scheme 1. This methodology has been successfully applied in our research group to the study of periodic systems such as single-walled carbon nanotubes,[24−26] polymers,[27] polypeptides,[28,29] and bulk actinide oxides.[30,31] As we show below, the bipolaronic lattice **ESI** in Scheme 1 is lower in energy than the polaronic lattices **ESI′** and **ESII**. Therefore, it should be responsible for the metallic behavior experimentally observed when **EB** is proton-doped. Indeed, the computed band structure for **ESI** is in good agreement with experimental data from absorption spectra.

It should be noted that the fully ionic picture in which the structures **ESI** and **ESI′** would correspond to a dicationic polymer chain with two Cl^- anions (counterions) and the structure **ESII** to a cationic polymer chain with one Cl^- anion (counterion) are particular cases of the models presented in Scheme 1. As we will show below, the analysis of the electron density corresponding to the wave function, solution of the Schroedinger equation for the systems under study, provides information about the final partial charges on the counterion ($Cl^{-\delta}$).

2. Computational Details

All calculations were carried out using the development version of the *Gaussian* suite of programs,[32] enabling geometry optimizations using periodic boundary conditions (PBC) with density functional theory (DFT)[33] methods and Gaussian basis sets.[34] Further details on this methodology can be found elsewhere.[19−23]

Pople's split-valence 6-31G(d,p) basis set[35] has been employed. To test the reliability of different functionals, we have carried out calculations using: (a) the LSDA Slater's local density exchange[36] plus the Vosko−Wilk−Nusair correlation functional V,[37] (b) the nonempirical Perdew−Burke−Ernzerhof (PBE)[38] functional which is a generalized gradient approximation (GGA),[39] and (c) the hybrid Perdew−Burke−Ernzerhof functional (PBEh)[40] which combines 25% of exact exchange with the PBE functional. Preliminary calculations indicated that 32 **k** points were enough to converge the energy to 10^{-8} au.

The DFT methodology has been shown to perform rather well in the study of radical, diradical,[41,42] and "multiradical"[30,31] systems. Furthermore, in the particular case of PANI several recent studies[14,15] on oligomer models demonstrated that DFT is able to provide structural and spectroscopic information fully consistent with the experimental data available.

The present methodology represents one step forward with respect to previous theoretical methods employed to study PANI,[11−16] in particular semiempirical approaches and oligomer models. As we will show below, some of the PBC/DFT geometrical and spectroscopic results are in good agreement with those reported in previous studies on oligomers.[14,15] However, the band gap structure which emerges in a straightforward manner from PBC calculations requires extrapolation techniques when estimated from the oligomer calculations. Our tools encompass the explicit consideration of the important electron correlation contributions and the appropriate treatment of a periodic system (polymer chain).

3. Results and Discussion

3.1. Equilibrium Geometries. Figure 1 shows the DFT-(PBC)/6-31G(d,p) optimized geometries for the structures involved in the mechanism presented in Scheme 1. Table 1

(19) Kudin, K. N.; Scuseria, G. E. *Chem. Phys. Lett.* **1998**, *283*, 61.
(20) Kudin, K. N.; Scuseria, G. E. *Chem. Phys. Lett.* **1998**, *289*, 611.
(21) Kudin, K. N.; Scuseria, G. E. *J. Chem. Phys.* **1999**, *111*, 2351.
(22) Kudin. K. N.; Scuseria, G. E. *Phys. Rev. B.* **2000**, *61*, 5141.
(23) Kudin,. K. N.; Scuseria, G. E. *Phys. Rev. B*, **2000**, *61*, 16440.
(24) Kudin, K. N.; Bettinger, H. F.; Scuseria, G. E. *Phys. Rev. B* **2001**, *63*, 045413.
(25) Barone, V.; Heyd, J.; Scuseria, G. E. *J. Chem. Phys.* **2004**, *120*, 7169.
(26) Barone, V.; Heyd, J.; Scuseria, G. E. *Chem. Phys. Lett.* **2004**, *389*, 289.
(27) Pino, R.; Scuseria, G. E. *J. Chem. Phys.* **2004**, *121*, 8113.
(28) Improta, R; Barone, V.; Kudin, K. N.; Scuseria, G. E. *J. Chem. Phys.* **2001**, *114*, 2541.
(29) Improta, R.; Barone, V.; Kudin, K. N.; Scuseria, G. E. *J. Am. Chem. Soc.* **2001**, *123*, 3311.
(30) Kudin, K. N.; Scuseria, G. E.; Martin, R. L. *Phys. Rev. Lett.* **2002**, *89*, 266402.
(31) Prodan, I.; Sordo, J. A.; Kudin, K. N.; Scuseria, G. E.; Martin, R. L. *J. Chem. Phys.* In press.
(32) Frisch, M. J.; et al. *Gaussian 01*, revisions A02, B01, and *Gaussian 03*, revisions B04, B07, development versions; Gaussian, Inc.: Pittsburgh, PA, 2001−2004.
(33) Koch, W.; Holthausen, M. C. *A Chemist's Guide to Density Functional Theory*, 2nd ed.; Wiley: Weinheim, Germany, 2000,
(34) Scuseria, G. E. *J. Phys. Chem. A* **1999**, *103*, 4782.
(35) Hehre, W. J.; Radom, L.; Schleyer, P. v. R.; Pople, J. A. *Ab initio Molecular Orbital Theory*; Wiley: New York, 1986.
(36) Slater, J. C. *Quantum Theory of Molecules and Solids*; McGraw-Hill: New York, 1974; Vol. 4.
(37) Vosko, S. H.; Wilk, L.; Nusair, M. *Can. J. Phys.* **1980**, *58*, 1200.
(38) (a) Perdew, J. P.; Burke, K.; Ernzerhof, M. *Phys. Rev. Lett.* **1996**, *77*, 3865. (b) Perdew, J. P.; Burke, K.; Ernzerhof, M. *Phys. Rev. Lett.* **1997** (E), *78*, 1396.
(39) Parr, R. G.; Yang, W. *Density Functional Theory of Atoms and Molecules*; Oxford University Press: New York, 1989.
(40) Ernzerhof, M.; Scuseria, G. E. *J. Chem. Phys.* **1990**, *110*, 5029−5036.
(41) Sullivan, M. B.; Brown, K.; Cramer, C. J.; Truhlar, D. G. *J. Am. Chem. Soc.* **1998**, *120*, 11779 and references therein.
(42) Lim, M. H.; Worthington, S. E.; Dulles, F. J.; Cramer, C. J. In *Density-Functional Methods in Chemistry*; ACS Symposium Series; Laird, B. B., Ross, R. B., Ziegler, T., Eds.; American Chemical Society: Washington, DC, 1996; Vol. 629, p 402.

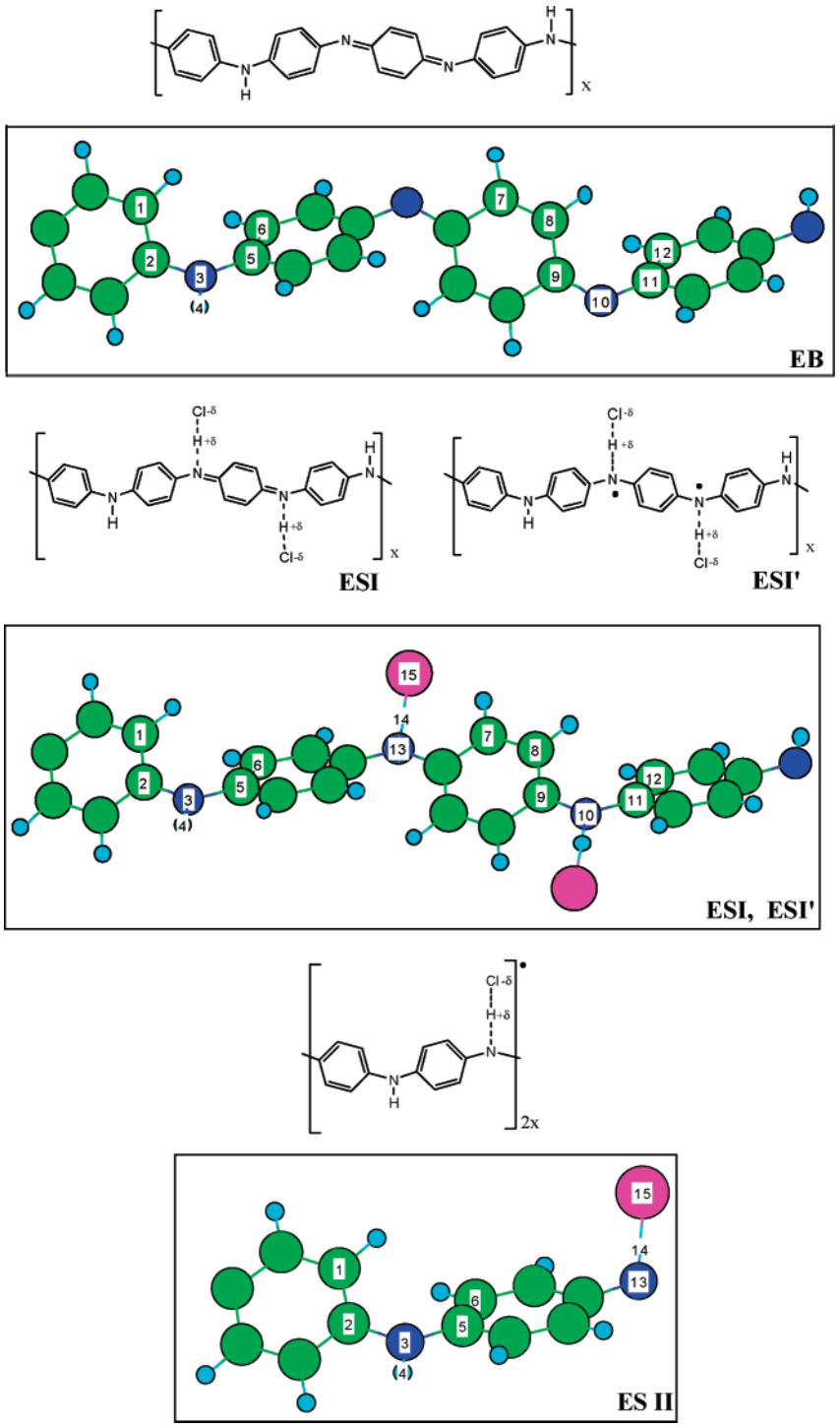

Figure 1. Emeraldine base (**EB**) and emeraldine salts: **ESI** (bipolaron), **ESI′** (polarons), and **ESII** (polaron).

collects the most representative geometrical parameters as estimated with the different functionals employed (LSDA, PBE, and PBEh). After exhaustive searches, the **ESI′** structure could not be located on the LSDA potential energy surface. As a general comment, all the functionals employed in this work led to quite similar geometrical predictions. Bearing in mind that the PBEh functional renders superior spectroscopic results (see below), the PBEh geometrical parameters will be used in the rest of the discussion.

In the case of **EB**, one of the rings exhibits a quinoidlike geometry with C—C bonds of 1.456(2) Å and C═C bonds of 1.349(1) Å, while the other three rings are benzenoid like with bond lengths of 1.398(11) Å [the *PBEh*/6-31G(d,p) C—C and C═C bonds in $C_6H_6N_2$ are 1.467 and 1.342 Å, respectively, and the carbon−carbon bond in C_6H_6 is 1.393 Å]. The carbon−nitrogen bonds of the two nitrogens attached to the quinoid ring (1.302 Å) are shorter than the rest of the carbon−nitrogen bonds in the structure [1.386(6) Å]. Therefore, the **EB** geometry is consistent with the formal structure represented in Scheme 1. An important feature of **EB** is the fact that while the π-electron delocalization energy favors all the C_6 rings to be in the same plane, the steric repulsions force the appearance of a torsional angle. Our theoretical calculations predict the four nitrogen atoms to be nearly coplanar (−0.3°−0.0°) forming tilt angles

Table 1. DFT(PBC)/6-31G(d,p) (DFT = LSDA, PBE, PBEh) Geometrical Parameters for **EB**, **ESI**, **ESI′**, and **ESII**. X−Y, X−Y−Z, and X−Y−Z−W Represent Distances, Angles, and Dihedral Angles, Respectively

system	geometry[a]	LSDA	PBE	PBEh
EB	C1−C2	1.403	1.413	1.401
	C2−N3	1.384	1.401	1.395
	N3−H4	1.021	1.017	1.007
	C8−C9	1.442	1.457	1.457
	C9−N10	1.319	1.329	1.302
	N10−C11	1.362	1.380	1.383
	C11−C12	1.415	1.426	1.409
	C2−N3−C5	129.3	129.8	128.9
	C9−N10−C11	123.2	123.7	123.6
	C1−C2−C5−C6	−37.3	−40.3	−43.6
	C8−C9−C11−C12	−40.7	−41.7	−42.3
	N−N−N−N	0.0	0.0	−0.3
ESI	C1−C2	1.403	1.414	1.401
	C2−N3	1.383	1.400	1.398
	N3−H4	1.023	1.019	1.009
	C8−C9	1.425	1.436	1.437
	C9−N10	1.337	1.352	1.324
	N10−C11	1.363	1.381	1.377
	C11−C12	1.411	1.422	1.409
	N13−H14	1.165	1.147	1.140
	H14−Cl15	1.679	1.733	1.721
	C2−N3−C5	129.3	129.8	128.9
	C9−N10−C11	130.8	130.0	130.4
	C1−C2−C5−C6	−37.1	−39.3	−42.8
	C8−C9−C11−C12	−29.1	−33.0	−32.5
	N−N−N−N	0.0	0.0	−0.6
ESI′	C1−C2		1.417	1.401
	C2−N3		1.394	1.399
	N3−H4		1.019	1.009
	C8−C9		1.423	1.406
	C9−N10		1.381	1.385
	N10−C11		1.377	1.347
	C11−C12		1.423	1.421
	N13−H14		1.085	1.119
	H14−Cl15		1.897	1.753
	C2−N3−C5		129.8	128.9
	C9−N10−C11		130.0	129.0
	C1−C2−C5−C6		−39.4	−43.0
	C8−C9−C11−C12		−34.8	−38.0
	N−N−N−N		0.0	−0.4
ESII	C1−C2	1.408	1.419	1.407
	C2−N3	1.376	1.392	1.386
	N3−H4	1.024	1.019	1.009
	N13−H14	1.126	1.094	1.141
	H14−Cl15	1.740	1.854	1.704
	C2−N3−C5	130.8	130.9	130.3
	C1−C2−C5−C6	−33.1	−36.1	−38.1

[a] Distances are given in angstroms, and angles, in degrees.

with the C_6 rings (from left to right in Figure 1) of 21.0°, −39.0°, 10.0°, and −37.2°, respectively. As expected,[43] these angles alternate in sign for adjacent rings along the chain to minimize steric repulsion between neighboring C_6 rings. MacDiarmid and co-workers modeled the emeraldine base geometry making no distinction between quinoid and benzenoid units and assuming geometrical parameters based on oligomer values.[43] Thus, the only variable in their model was the ring tilt angle. These authors reported that the relative intensities of the X-ray reflections depend strongly on this angle. They found that a value of about 30° leads to the best fit to the experimental data. Our calculations show that the situation is much more complex than in the simplified model employed by MacDiarmid and co-workers. The present theoretical geometries could be useful to try new fittings.

The proton-doping of **EB** leads to the structure **ESI** where three rings remain benzenoid structures with carbon−carbon bonds of 1.398(14) Å and the fourth ring is a quinoid structure with C═C and C−C bonds of 1.440(4) and 1.356 Å, respectively. The HCl molecule interacts with **EB** forming two hydrogen bonds with an N···H distance of 1.140 Å. The H···Cl interacting distance becomes 1.721 Å (to be compared with the *PBEh*/6-31G(d,p) H−Cl bond length in hydrogen chloride: 1.281 Å).

The four nitrogen atoms remain almost coplanar (−0.6−0.0°) as in **EB**, and the tilt angles with the C_6 rings (from left to right in Figure 1) become 27.3°, −26.0°, 10.5°, and −25.1°, respectively. Bearing in mind the relationship between π-conjugation and electrical conductivity, the closer these angles are to each other (in absolute value) and the closer they are to zero, the greater the electrical conductivity should be. Therefore, we conclude that the notable reduction of two of the torsional angles when passing from **EB** to **ESI** suggests a greater conjugation and, consequently, an increase in conductivity (see below the band gap analysis). Using a rather simplified model for the geometry, MacDiarmid and co-workers concluded in their X-ray study on polyaniline that the ring torsion should decrease to a value 0°−15° for the emeraldine salt.[43] The geometrical parameters from the present calculations might be useful to carry out a more confident fitting with the X-ray experimental data. On the other hand, the theoretically predicted unit cell length for **ESI** (20.8 Å) matches twice the experimental value based on a half-size cell.[43] Therefore, the 1-D model adopted in the present study is fully compatible with the experimental observation.

The transformation of the bipolaron lattice **ESI** into the polarons **ESI′** parallels the conversion of the quinoid like ring in **ESI** into a more benzenoid form in **ESI′** with carbon−carbon bonds of 1.400(19) Å. The N···H and H···Cl interaction distances are 1.119 and 1.753 Å, suggesting a slightly stronger interaction with the doping acid than in the case of **ESI**.

As in **EB** and **ESI**, the four nitrogen atoms are almost coplanar in **ESI′** (−0.4°−0.0°). Although two of the tilt angles increase (one of them in a remarkable way), the notable reduction of the other two tilt angles favors the conjugation (see below the band gap analysis).

Finally, the geometrical parameters of the polaron lattice **ESII** remain rather similar to the corresponding ones in the **ESI′** polaron lattice (see Table 1). The proton interaction becomes a little bit weaker (the N13−H14 distance in Figure 1 increases slightly), and the tilt angles between the plane defined by three nitrogen atoms (one of them in the next cell) become 21.8° and −21.4°, respectively. These relatively small and very similar angles suggest an efficient conjugation that should lead to an increase in electrical conductivity (see below the band gap analysis). The theoretically predicted unit cell length for **ESII** (10.2 Å) is in good agreement with the experimentally estimated value (10.4 Å).[43]

Natural bond orbital (NBO)[44] analyses and Bader-type calculations[45] show that, as expected, the counterions become rather ionic. Charges of about −0.7e (NBO) or −0.75 e (Bader) on every chlorine and +0.7e (NBO) or +0.75 e (Bader) (per chlorine) delocalized over the corresponding chains are close to MacDiarmid and co-workers' formal representation[16] of a positively charged chain (monocationic in the case of **ESII** and

(43) Pouget, J. P.; Józefowicz, M. E.; Epstein, A. J.; Tang, X.; MacDiarmid, A. G. *Macromolecules* **1991**, *24*, 779.

(44) Reed, A. E.; Curtiss, L. A.; Weinhold, F. *Chem. Rev.* **1988**, *88*, 899.

(45) Bader, R. F. W. *Atoms in Molecules. A Quantum Theory*; Oxford University Press: New York, 1989.

Table 2. DFT(PBC)/6-31G(d,p) Total Energies (*E*; au) and Entropies (*S*; cal mol^{-1} K^{-1}) for **EB**, **HCl**, **ESI**, **ESI′**, and **ESII** Structures as Computed with the LSDA, PBE, End PBEh Functionals; Electronic (ΔE; kcal mol^{-1}) and Entropic ($-T\Delta S$; kcal mol^{-1}) Energy Contributions for the Formation of **ESI** and **ESI′** [**EB** + 2HCl → **ESI** (or **ESI′**)] and **ESII** [**EB** + 2HCl → 2**ESII**] Are Also Given

functional	system	energy	S^a	ΔE	$-T\Delta S^b$
LSDA	EB	−1134.283 196	167.0		
	HCl	−459.282 583	44.63		
	ESI	−2052.939 555	190.6	−57.2	19.6
	ESI′				
	ESII	−1026.457 164	122.2	−41.4	18.0
PBE	EB	−1142.997 629	168.2		
	HCl	−460.591 482	44.62		
	ESI	−2064.239 312	193.4	−36.8	19.1
	ESI′	−2064.222 138	197.4	−26.1	17.9
	ESII	−1032.109 367	124.3	−23.9	16.9
PBEh	EB	−1143.077 781	165.8		
	HCl	−460.631 044	44.59		
	ESI	−2064.389 364	188.9	−31.1	19.7
	ESI′	−2064.374 314	193.6	−21.6	18.3
	ESII	−1032.185 089	120.5	−19.0	17.6

[a] Entropies were estimated from the corresponding H-capping four-ring oligomers. [b] $T\Delta S$ was estimated from the monomer structure at 298.15 K.

dicationic for **ESI** and **ESI′**) and one (**ESII**) or two (**ESI**, **ESI′**) negatively charged chlorine counterions in the hollows of the polymer zigzag.[43]

3.2. Energies. Table 2 collects the total energies for the systems under study obtained at the DFT(PBC)/6-31G(d,p) (DFT = LSDA, PBE, PBEh) level of theory. The entropy contributions, also included, were estimated within the ideal gas, rigid rotor, and harmonic oscillator approximations.[46] To keep the required frequency calculations within practical limits, H-capping four-rings oligomer models were used for the **EB**, **ESI**, **ESI′**, and **ESII** structures. Analytical methods for the evaluation of the Hessian matrix are not available for PBC calculations at present.[32] A temperature of 298.15 K and a pressure of 1 atm were assumed.

While the entropic destabilizations are rather similar as estimated with the different functionals, there are substantial variations in the computed total energy stabilizations. The LSDA values are about 20−25 kcal/mol lower than the corresponding ones estimated with the more realistic PBEh functional, which includes a portion of Hartree−Fock-type exact exchange. The differences between PBE and PBEh relative energy predictions (about 5 kcal/mol) are much less pronounced. Interestingly, quite similar relative electronic energy stabilization of **ESI** with respect to **ESII** (or **ESI′**) is predicted by the three functionals: −15.8, −12.9, and −12.1 (−, −10.7, and −9.5) kcal/mol for LSDA, PBE, and PBEh, respectively.

Heeger and co-workers[6] speculated that the driving force for converting **ESI** to **ESI′** in a mechanism like the one in Scheme 1 is expected to be provided by the gain in resonance energy obtained in going from a quinoneimine to a diaminobenzene. The present calculations show that **ESI′** is less stable than **ESI** by about 10 kcal/mol. Furthermore, the formation of the **ESII** polaron lattice is, according to the data in Table 2, disfavored when considering total energies. The entropic contributions are similar for the three structures considered: **ESI**, **ESI′**, and **ESII**. Although they slightly favor the latter (by about 1−2 kcal/mol), it is not enough to make **ESII** more stable than **ESI**. Therefore, the present calculations suggest that the bipolaronic lattice **ESI** is the most stable structure, independently of the DFT functional employed, and should be responsible for the notable increase in electrical conductivity when doping **EB** with HCl.

The relative stability of polarons and bipolarons in conjugated polymers is an open question. Different theoretical methods lead to opposite conclusions.[18,47−50] One of the most recent studies has been that reported by de Oliveira and dos Santos[51] who employed AM1[52] and ZINDO-S/CI[53] semiempirical Hamiltonians. These authors concluded that the bipolaron creation energy exceeds that involved in the creation of a pair of polarons. Their results were consistent with the coexistence of polarons and bipolarons in short oligomers and the predominance of polarons in long chains. The reported ZINDO-S/CI UV−visible absorption bands were in good agreement with experimental absorption spectra of several emeraldine oligomers.[54]

While the good performance of methods such as ZINDO-S/CI to predict UV−visible absorption spectra in organic systems cannot be disputed, the AM1 energy analysis, which contrasts with the present DFT-PBC/6-31G(d,p) predictions, is questionable. It should be also stressed at this point that the ab initio calculations presented in this work do explicitly include the effect of the counterions ($Cl^{-\delta}$) in the doped emeraldine. Their screening effect on the Coulomb repulsion between the two positive charges in the bipolaron defects must be an important factor in order to determine their relative stability with respect to polaron defects.[17,47,51,55]

Apart from the good agreement with the experimental bands of the visible absorption spectra, which as we will show below are also compatible with a bipolaron structure in doped **EB**, MacDiarmid and co-workers[16] based their preference for the polaron lattice on the far-infrared activity of the optical absorption spectra that is interpreted as intraband absorption at low frequency. The band structure of a polaron defect provided by the VEH simple model[16] with a half-occupied polaron band supports the far-infrared absorption. However, at the DFT-PBC level, only the LSDA local density and PBE generalized gradient functionals generate density of states (DOS) are compatible with intraband absorptions for the polaronic structure **ESII** (but not for the other polaronic structure **ESI′** which presents a gap between the valence and conduction bands) (see Figure 2). The more sophisticated and generally more accurate PBEh functional renders DOSs exhibiting gaps between the valence and conduction bands for both polaron and bipolaron structures (see Figures 4−6). It should also be pointed out that the VEH approach has been reported to fail in reproducing the optical properties of **EB**.[13] Such a poor performance has been attributed to the one-electron nature of the VEH formalism.

MacDiarmid and co-workers[16] have also mentioned the evolution of the magnetic data upon protonation in support of the polaron lattice model for PANI. However, several ESR, EPR,

(46) McQuarrie, D. A. *Statistical Thermodynamics*; University Science Books; Mill Valley: CA, 1973.
(47) Brédas, J. L.; Thémans, B.; Fripiat, J. G.; André, J. M.; Chance, R. R. *Phys. Rev. B* **1984**, *29*, 6761.
(48) Shimoi, Y.; Abe, S. *Phys. Rev. B* **1994**, *50*, 14781.
(49) Brazovskii, S.; Kirova, N.; Yu, Z. G.; Bishop, A. R.; Saxena, A. *Opt. Mater.* **1998**, *60*, 781.
(50) Kuwabara, M.; Shimoi, Y.; Abe, S. *J. Phys. Soc. Jpn.* **1998**, *67*, 1521.
(51) de Oliveira, Z. T. Jr.; dos Santos, M. C. *Solid State Commun.* **2000**, *114*, 49.
(52) Dewar, M. J. S.; Zoebish, E. G.; Healy, E. F.; Stewart, J. J. P. *J. Am. Chem. Soc.* **1985**, *107*, 3902.
(53) Zerner, M. C. *Quantum Theory Project, ZINDO*; University of Florida: Gainesville, FL 32611.
(54) Sadighi, J. P.; Singer, S. L.; Buchwald, S. L. *J. Am. Chem. Soc.* **1998**, *120*, 4960.
(55) Kahol, P. K.; Spencer, W. R.; Pinto, N. J.; McCormick, B. J. *Phys. Rev. B* **1994**, *50*, 18647.

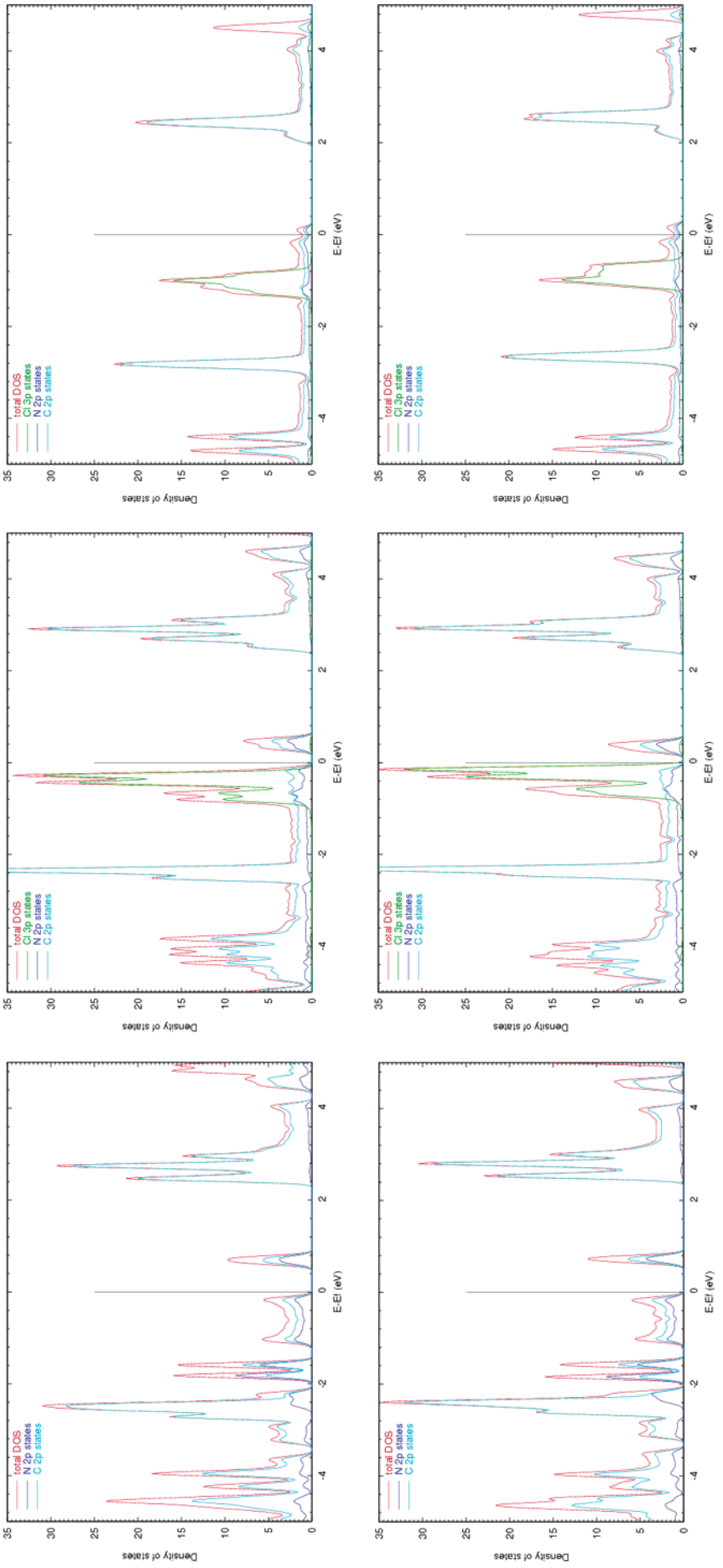

Figure 2. Density of states for the **EB**, **ESI**, and **ESII** structures as computed with the LSDA (first row) and PBE (second row) functionals.

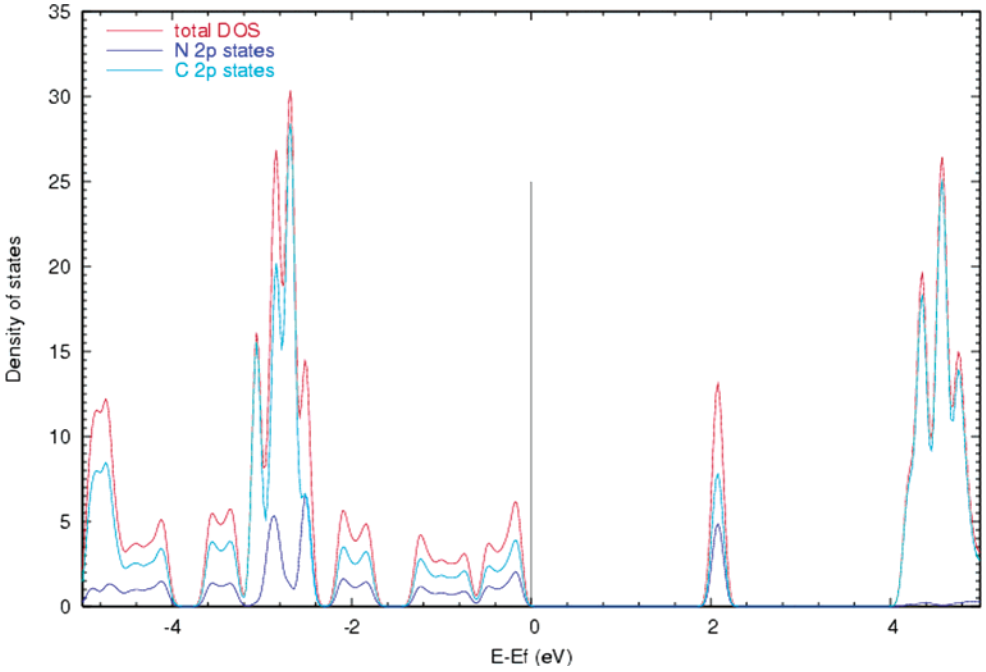

Figure 3. PBEh density of states for **EB**.

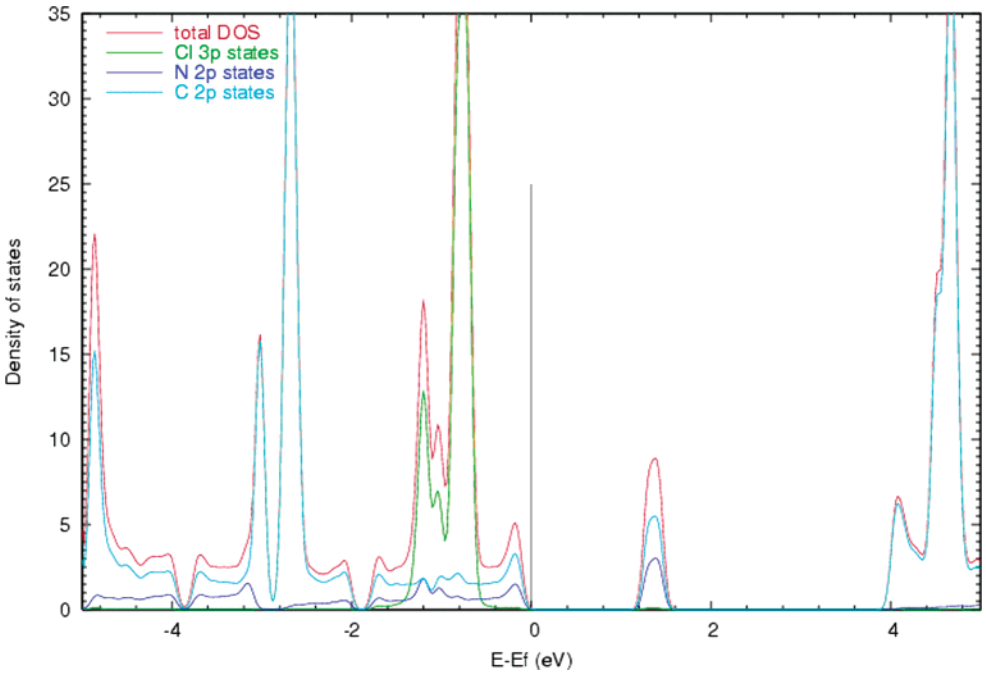

Figure 4. PBEh density of states for **ESI**.

and cyclic voltammetric studies do not discard the presence of bipolaronic lattices in doped **EB**.[55−58]

3.3. Density of States. Figures 2−6 depict the DOS curves for the structures involved in the mechanism under study to explain the spectacular increase in the electrical conductivity of PANI by acid−base chemistry. The total DOSs are broken down into atomic orbital components (2p-C, 2p-N, and 3p-Cl) within the Mulliken population analysis approximation.

In what follows, the absorption bands are going to be estimated from the DOSs curves without accounting for orbital relaxation effects. Kwon and McKee have shown recently[14] that the HOMO−LUMO energy difference provides a very good estimate of the band gaps.

In general, the LSDA and PBE DOSs (Figure 2) look very similar to each other and differ substantially from the PBEh DOSs (Figures 3−6).

Figure 2 (LSDA and PBE functionals) suggests that one absorption band should be observed in the **EB** photoemission spectrum at about 0.9 eV. A second rather broad band extending from 2.4 to 4.1 eV is also theoretically predicted. The PBEh functional (see Figure 3) locates the first peak at about 2.2 eV,

(56) Libert, J.; Cornil, J.; dos Santos, D. A.; Bredas, J. L. *Phys. Rev. B* **1997**, *56*, 8638.
(57) Lippe, J.; Holze, R. *Synth. Met.* **1991**, *43*, 2927.
(58) Tang, J.; Allendoerfer, R. D.; Osteryoung, R. A. *J. Phys. Chem.* **1992**, *96*, 3531.

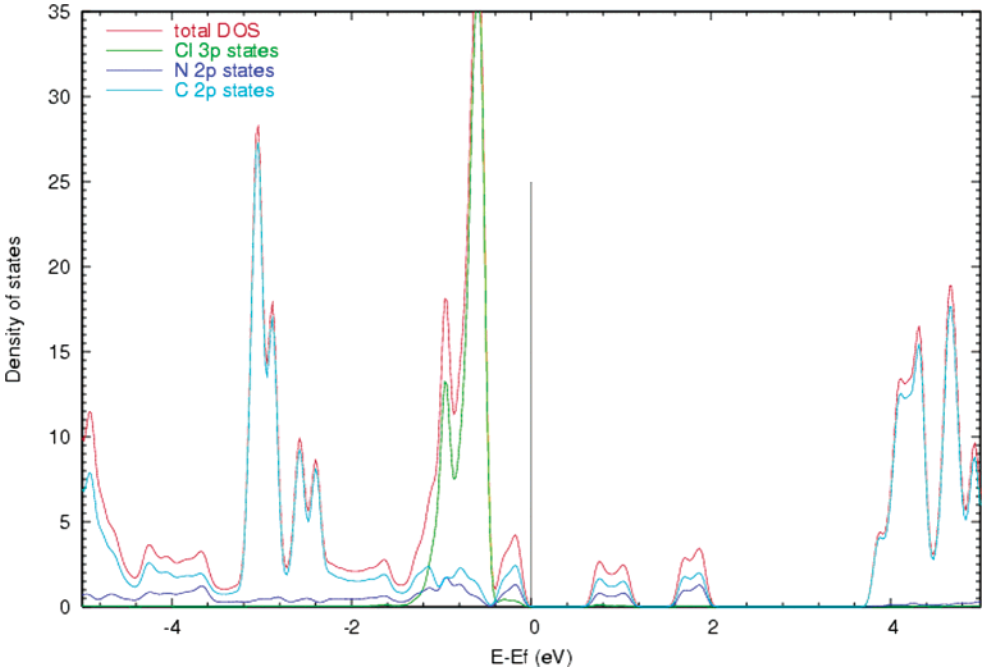

Figure 5. PBEh density of states for **ESI′**.

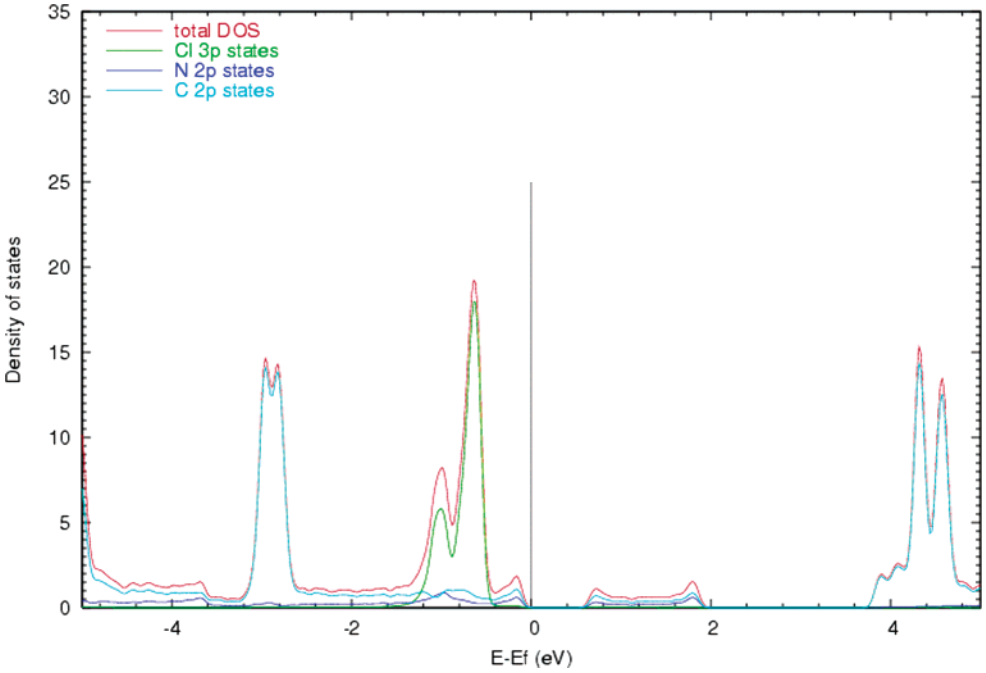

Figure 6. PBEh density of states for **ESII**.

and the broader band starts at about 4.0 eV. This latter prediction agrees much better with the experimental optical absorption measurements of the polymeric **EB** base (in film form or in solution) which shows the presence of two bands at about 2 and 3.6−3.8 eV, respectively.[8,59] The first band involves the highest occupied crystal orbital (HOCO) and the lowest unoccupied crystal orbital (LUCO). A graphical analysis of the orbitals corresponding to the Γ-point shows that the HOCO results from a combination of 2p orbitals of carbon and nitrogen atoms (see also Figure 3). All the rings and nitrogen π-orbitals present significant contributions, thus showing bonding−antibonding patterns characteristic of aromatic systems.

The LUCO shows smaller contributions from the benzenoid rings as compared with the quinoid ring. Therefore, our results support the assignment of this band to a charge-transfer exciton-like transition between benzenoid and quinoid rings.[15]

Figure 3 shows that the second band involves the HOCO and the LUCO + 1 with almost no contributions from the nitrogen 2p orbitals. The graphical analysis shows that this LUCO + 1 exhibits π^* characteristics delocalized over all the C_6 rings. Therefore, it can be assigned to a $\pi-\pi^*$ band gap absorption, in agreement with the experimental observation.[15]

(59) Leng, J. M.; McCall, R. P.; Cromack, K. R.; Sun, Y.; Manohar, S. K.; MacDiarmid, A. G.; Epstein, A. J. *Phys. Rev. B* **1993**, *48*, 15719.

Transformation of **EB** into **ESI** implies a notable reduction of the first band gap. Again, the LSDA and PBE functionals lead to the prediction of a much lower absorption band (about 0.4 eV) than the PBEh functional (about 1.6 eV; see Figure 4), and interestingly this latter prediction is fully compatible with the experimental observed optical transition for emeraldine salt at 1.5 eV.[8,16] A graphical analysis of the two orbitals involved in the first absorption band shows that both of them (HOCO and LUCO) represent typical bonding−antibonding patterns of aromatic systems with contributions of the π-ring and π-nitrogen orbitals. The 3p chlorine orbitals contribute predominantly to the HOCO − 1. The experimentally observed optical transition at 2.8 eV that is associated with the HOCO − 1 → LUCO transition by MacDiarmid and coworkers[16] agrees rather well with the PBEh energy difference between the huge peak at −0.8 eV mostly arising from chlorine 3p states (counterions) and the first peak above the Fermi level (at about 1.4 eV). Also, the optical absorption at 4.1 eV is in excellent agreement with the PBEh energy difference between the peak close to the Fermi level and the first peak of the band starting at about 4 eV. Therefore, the PBEh DOS is fully compatible with the three experimentally observed transitions for doped **EB**.

A polaron-like lattice (**ESI′**), geometrically close to **ESI**, would imply (see Figure 5) the appearance of two small bands at approximately 0.9 and 1.8 eV. In any case, the energetic analysis carried out in the previous section strongly suggests that the formation of the **ESI′** structure is disfavored with respect to **ESI**.

On the other hand, the polaron lattice **ESII** should lead, according to the LSDA and PBE results (see Figure 2), to a virtually metallic behavior with a practically inexistent first band gap, and a second very broad band extending from 2.0 to 4.4 eV with a prominent peak at about 2.5 eV. The PBEh hybrid functional (see Figure 6) predicts the existence of a broad polaron band extending from 0.6 to 2.0 eV that should be responsible for the optical absorption band of protonated emeraldine at 1.5 eV with a bandwidth of about 1 eV.[16] The transition involving the peak at about −0.6 eV (exhibiting predominantly Cl 3p character) and the broad conduction band (0.6−2.0 eV) should be associated with the experimental 2.8 eV transition. Finally, the PBEh theoretical transition involving the peak closest to the Fermi level (about −0.2 eV), and the first peak of the complex band starting at about 3.7 eV should be responsible for the optical transition observed at 4.1 eV.

According to the analysis presented above, both the **ESI** bipolaron lattice and the **ESII** polaron lattice give rise to DOSs that agree reasonably well with the optical absorption spectra of protonated PANI. However, we have shown that DFT calculations, using the hybrid PBEh functional and periodic boundary conditions, clearly indicate that the bipolaronic structure is more stable.

Heeger[4] has stressed that the electrical conductivity results from the existence of charge carriers (through doping) and from the ability of these charge carriers to move along the π-band "highway" (conjugation). The analysis of the geometries in a previous section and the DOSs above lead us to the conclusion that the **ESI** bipolaronic structure, which conjugates both factors, is a suitable candidate to rationalize the metallic final state of polyaniline upon proton-doping.

Other potentially influential factors such as the degree of doping,[48,58,60−63] disordered distribution of the symmetric or asymmetric bipolarons,[64,65] or interchain interactions[17,59] should be further explored at the same level of theory employed in the present paper, and work along those lines is in progress.

4. Conclusions

The doping of polyaniline by acid−base chemistry has been studied by means of ab initio DFT calculations with periodic boundary conditions and a 6-31G(d,p) basis set. Three funtionals (LSDA, PBE, and PBEh) were here employed. All the structures involved in the mechanism proposed by MacDiarmid and coworkers to explain the electrical conductivity increase observed when the emeraldine base is proton-doped, have also been considered: the emeraldine base (**EB**), the bipolaron lattice formed after proton-doping (**ESI**), the two polaron lattice obtained from the quinoid-to-benzenoid transformation in **ESI** (**ESI′**), and, finally, the polaron lattice arising from the separation of the two polarons in **ESI′** (**ESII**).

The PBEh calculations lead to spectroscopic parameters in much better agreement with the available experimental data than the corresponding LSDA and PBE predictions. This conclusion is supported by other recent studies in our research group on different chemical species.

The fully optimized geometries **EB**, **ESI**, **ESI′**, and **ESII** are consistent with those foreseen in MacDiarmid and co-workers' mechanism. The computed torsional angles among the different C_6 rings in those structures are consistent with the corresponding structural information derived from X-ray data.

The computed energies indicate that the bipolaronic lattice **ESI** is more stable than the rest of the structures and, consequently, should be responsible for the properties exhibited by the proton-doped emeraldine base, particularly, its conductivity.

The PBEh density of states for emeraldine base **EB** show the presence of two band gaps of about 2.2 and 4.0 eV, respectively, which agree rather well with the experimentally observed absorptions at about 2 and 3.8 eV. The analysis of the different contributions to the crystal orbitals involved in these absorptions suggest the first one to be a charge-transfer exciton-like transition between benzenoid and quinoid rings and the second one to represent a traditional $\pi-\pi^*$ transition, in agreement with previous assignments from the experimental data.

The PBEh density of states for emeraldine salt **ESI** is compatible with optical transitions at about 1.6, 2.2, and 4.1 eV, which agree rather well with the optical absorption spectra of protonated PANI, exhibiting peaks at 1.5, 2.8, and 4.1 eV.

Acknowledgment. Helpful discussion on the use of the Periodic Boundary Conditions algorithm with Drs. I. Prodan, K. N. Kudin, and R. L. Martin are greatly appreciated. Partial financial support from DGES (Madrid, Spain) under Projects BQU-3660-C02-01 and BQU-07405-C02-02 is also acknowl-

(60) Kaya, M.; Kitani, A.; Sasaki, K. *Chem. Lett.* **1986**, 147.
(61) Jozefowicz, M. E.; Laversanne, R.; Javadi, H. H. S.; Epstein, A. J.; Pouget, J. P; Tang, X.; MacDiarmid, A. G. *Phys. Rev. B* **1989**, *39*, 12958.
(62) Nechtschein, M.; Genoud, F.; Menardo, C.; Mizoguchi, K.; Travers, J. P.; Villeret, B. *Synth. Met.* **1989**, *29*, E211.
(63) Zuo, F.; Angelopoulos, M.; MacDiarmid, A. G.; Epstein, A. J. *Phys. Rev. B* **1989**, *39*, 3570.
(64) Galvao, D. S.; dos Santos, D. A.; Laks, B.; de Melo, C. P.; Caldas, M. J. *Phys. Rev. Lett.* **1989**, *63*, 786.
(65) Lavarda, F. C.; dos Santos, D. A.; Galvao, D. S.; Laks, B. *Phys. Rev. Lett.* **1994**, *73*, 1267.

edged. J.A.S. thanks MEC (Madrid, Spain) for financial support to spend several months at Rice University where the present study started. The work at Rice University was supported by the U.S. National Science Foundation and The Welch Foundation.

Supporting Information Available: Full ref 32 and Cartesian coordinates for all the structures. This material is available free of charge via the Internet at http://pubs.acs.org.

JA051012T